2010 IEEE International Conference on Robotics and Automation
Anchorage Convention District
May 3-8, 2010, Anchorage, Alaska, USA

Analysis on a Friction Based "Twirl" for Biped Robots

Kanako Miura, Shin'ichiro Nakaoka, Mitsuharu Morisawa
Fumio Kanehiro, Kensuke Harada, and Shuuji Kajita

Abstract— **This paper presents preliminary results and analysis on generating turning motion of a humanoid robot by slipping the feet on the ground. Humans unconsciously exploit the fact that our feet slip on the ground; such slip motion is necessary for humanoids so as to realize sophisticated human-like motions. In order to generate the slip motion, we need to predict the amount of slip. We propose the hypothesis that the turning motion is caused by the effect of minimizing the power generated by floor friction. A model of rotation by friction force is described on the basis of our hypothesis. The case that a robot applies the same force on both feet is discussed; then, we extend the discussion to the case of different force distribution. The hypothesis is verified through experiments with a humanoid robot HRP-2.**

I. INTRODUCTION

In our daily life, we unconsciously exploit the fact that our feet slip on the ground, when we turn or stop. However, most current humanoid robot locomotion assumes no slip contacts. As a result, robots tend to take many small steps when turning in place, which usually takes a considerable time to complete the turning motion. Taking all these steps does not seem effective in terms of both energy consumption and stability. Therefore, we believe that the use of slip is important for realizing quick and smooth robot motion. This paper presents a preliminary discussion of the slip phenomenon, aiming to realize the performance of highly sophisticated human-like motion by humanoid robots.

The topics related to our final goal are as follows: elucidating the slip phenomenon in turning motion, creating a model that predicts the amount of slip, and the realization of twirling motion of a humanoid robot by exploiting slip.

In the field of ergonomics and biomechanics, intensive research has been performed on analyzing slipping and slip induced in a fall[1][2][3]. However, there still exists some controversy on the conditions that result in falling[4].

Conventional studies on biped locomotion in a low friction environment mainly focus on the prediction, avoidance, or recovery from slip. Boone and Hodgins[5][6] simulated a running biped on a floor with a low friction area by introducing a reflex control strategy. Park and Kwon[7] designed a controller to enlarge the frictional force on the occurrence of slipping, and simulated a 12-DOF biped robot walking on slippery surface. Kajita et al.[8] described a calculation of ZMP[9] concerning slip. Though ZMP is useful to check the possibility of a robot falling down, the conventional way to calculate ZMP cannot be used in case of slip. It provides a good prediction of falling caused by slipping. Kajita et al. also successfully demonstrated a walk on a low friction environment using a humanoid robot HRP-2[10]. Kaneko et al.[11] proposed a slip observer to stabilize a biped walking on a slippery floor. Zhu[12] proposed a method to predict the most possible slipping direction including rotation of a support foot during a single support phase.

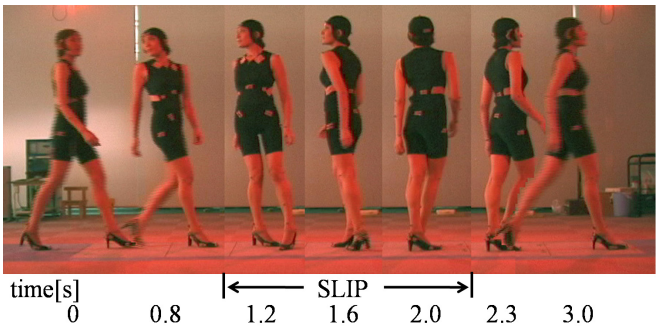

Fig. 1. 360-deg turn by a professional walking model (the model belongs to Walking Studio Rei)

There exists some studies that have addressed the issues regarding the proactive use of slip for humanoid motion. Nishikawa[13][14] proposed a mechanical method to use slip for biped robots by adding a piston to the heel of the foot in order to generate rotational slip. Although the proposed mechanism is based on the concept of generating friction torque, the physical model is not numerically revealed. There also exists a study conducted by Koeda et al.[15] on the application of slip to the turning motion of a small humanoid robot HOAP-2. The robot pivots the feet one by one, keeping contact with the floor, instead of lifting them. Koeda claims that the robot can maintain a large support polygon while turning. The proposed motion used point contact between one corner of the pivoting foot and the ground for realizing 90-deg turning motion. Further, Koeda et al.[16] compared 30-deg turning motion between two cases. In one case, the mass load of the robot's body was applied uniformly on both soles, and in the other case, it was concentrated on opposing corners of the soles. Koeda claims that the corners do not slide much when the load is concentrated on the corners.

A preliminary discussion of the slip phenomenon has already been made and our hypothesis has been demonstrated with a humanoid robot platform HRP-2[17]. However, the hypothesis is inaccurate in some cases. In this paper, we

All authors are with Humanoid Research Group, Intelligent Systems Research Institute, National Institute of Advanced Industrial Science and Technology, Tsukuba 305-8568, Japan. {kanako.miura, s.nakaoka, m.morisawa, f-kanehiro, kensuke.harada, s.kajita}@aist.go.jp

correct the inaccuracy and extend the hypothesis to the case where the mass load of the robot's body is applied asymmetrically on the right and left soles.

Figure 1 shows a photograph sequence of a professional walking model performing a 360-deg turn. By slipping the soles of both feet, she turns speedily and smoothly. Setting our sights on this motion, we investigate the fundamental properties of rotational slip during a twirl.

In order to realize the desired twirling motion, the relation between a robot motion and the resulting angle is investigated in this paper. We intend to achieve a better understanding of the phenomenon of rotational slip through this study.

II. SLIP MODEL

In this section, a model of rotation caused by friction force is proposed. As shown in Fig. 2, a humanoid robot can be modeled as a set of rigid bodies. We define the robot's base frame on the pelvis as Σ_B. It is assumed that the center of mass is coincident with the origin of Σ_B so as to simplify the model. At the start of a motion, the projection of the base frame on the floor and the world frame Σ_W are exactly the same. Our assumption is that the robot's body will rotate from the reaction force when the robot moves its feet, as shown in Fig. 3. We define θ to be the angle between the world frame and the robot's base frame. When the robot moves, we expect θ to increase.

We make a hypothesis that the turning motion is caused by the effect of minimizing the power generated by floor friction. In order to simplify the model, we adapt the following assumptions. These assumptions are also used in researches on robot manipulation[18][19].

1) The motions are quasi-static; in other words, the motions are slow enough that frictional forces dominate inertial forces.
2) The dynamic and the static coefficients of friction acting between the feet and the floor are equal.
3) The plane of the floor is uniform and horizontal, and the friction distribution on the sole of the foot does not change.

According to assumption 1, we consider the twirling motion caused only by the mechanistic effect of the lower body motion. The turning motion realized using the momentum of the entire body will be covered in a future study. Further, we also assume that the robot applies the same weight on the right and left feet, uniformly. The case of an asymmetric load applied to each foot will be discussed later in this paper.

A. Symmetric load on both feet

First of all, our hypothesis is that the turning motion is caused by the effect of minimizing the power generated by floor friction.

$$\omega(t) = argmin\{\mathcal{P}(\omega(t))\} \tag{1}$$

where ω denotes the angular velocity of the robot, and $\mathcal{P}$ is the total power generated on the both soles. According to the above assumptions, the axis of rotation of the robot is

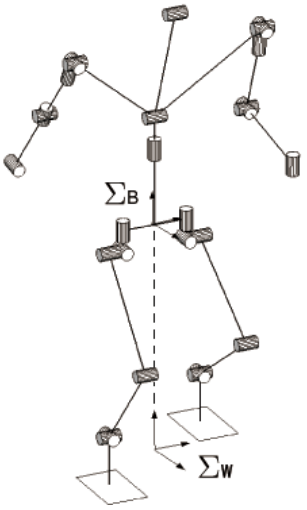

Fig. 2. Model of a robot, its base frame, and world frame. The origin of the base frame is fixed on the waist link of the robot, and the origin of the world frame is its projection on the floor at the start of the robot's motion.

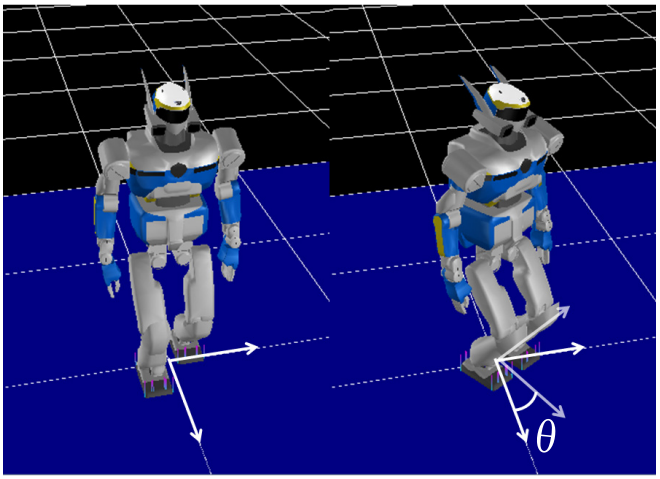

Fig. 3. Motion of a robot and the definition of rotational angle θ. Left: robot at the start of the execution of a motion. Right: robot at the end of the motion.

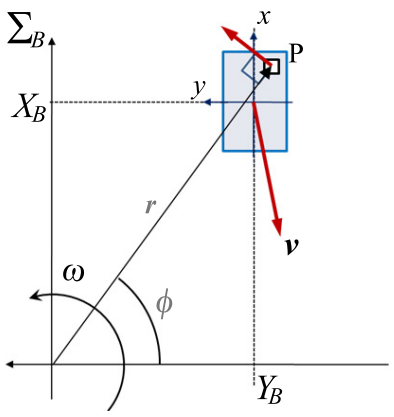

Fig. 4. Right-foot position and its instant velocity in the base frame.

coincident with the z-axis of the base frame. Therefore, the angular velocity vector is $\boldsymbol{\omega} = (0, 0, \omega)$.

In Fig. 4, the motion of the right foot is shown for explaining the hypothesis. Power can be presented as a time-derivative of the mechanical work done on the floor.

$$\mathcal{P} = \frac{d\mathcal{W}}{dt} \tag{2}$$

where $\mathcal{W}$ represents the work done by the both sole on the floor, and t is the time.

The work $\mathcal{W}$ is expressed as the product of the frictional force multiplied by the displacement of all points on the both soles of the robot. The point P is on the sole of a foot, and it is at distances of x and y from the center of the sole in the longitudinal and lateral directions. The center of the sole is X_B apart along the x-axis, and Y_B apart along the y-axis of the base frame. The robot moves its feet with velocity $\boldsymbol{v}$ in the base frame. Since the reaction force causes the robot to rotate, the point P also has velocity $\boldsymbol{\omega} \times \boldsymbol{r}$, where $\boldsymbol{r}$ is the position of the point P with respect to the origin of the base frame. Thus, the point P slides with velocity V, which is the resultant vector of $\boldsymbol{v}$ and $\boldsymbol{\omega} \times \boldsymbol{r}$.

The work done on P can be calculated by multiplying the frictional force f applied to a small area at P by the sliding displacement expressed by the time integration of V:

$$\begin{aligned} \mathcal{W}_P &= \int f|V|dt \\ &= f\int|V|dt \\ &= \frac{\mu Mg}{2l_x l_y}\int|\boldsymbol{v} + \boldsymbol{\omega} \times \boldsymbol{r}|dt \end{aligned} \tag{3}$$

where f indicates the frictional force per unit area, l_x and l_y denote the length and width of the sole, and μ, M, and g represent the friction coefficient, the total mass of the robot, and the gravity coefficient, respectively. In practice, since the applied normal force is always equal to f all through the motion, we obtain (3).

By integrating over the area of a sole and according to assumption 3, we obtain an expression for the total work at the sole:

$$\begin{aligned} \mathcal{W}_{right} &= \int_{-\frac{l_y}{2}}^{\frac{l_y}{2}}\int_{-\frac{l_x}{2}}^{\frac{l_x}{2}} \mathcal{W}_P \; dxdy \\ &= \frac{\mu Mg}{2}\int_{-\frac{l_y}{2}}^{\frac{l_y}{2}}\int_{-\frac{l_x}{2}}^{\frac{l_x}{2}}\int|V|dt \; dxdy \end{aligned} \tag{4}$$

where,

$$\begin{aligned} |V| &= \sqrt{V^2}dxdy \\ &= \sqrt{V_{X_B}^2 + V_{Y_B}^2} \\ &= \sqrt{|\boldsymbol{v} + \boldsymbol{\omega} \times \boldsymbol{r}|^2} \\ &= \sqrt{\{v_x - \omega r cos(\phi)\}^2 + \{v_y + \omega r sin(\phi)\}^2} \\ &= \sqrt{\{v_x - \omega(Y_B + y)\}^2 + \{v_y + \omega(X_B + x)\}^2} \end{aligned} \tag{5, 6}$$

where r denotes the norm of $\boldsymbol{r}$, and v_x and v_y represent the velocity components along the x- and y-axes of the base frame, respectively. Then, the loss of power on the right sole can be obtained as the time-derivative of $\mathcal{W}_{right}$:

$$\begin{aligned} \mathcal{P}_{right} &= \frac{d}{dt}\mathcal{W}_{right} \\ &= \frac{\mu Mg}{2}\int_{-\frac{l_y}{2}}^{\frac{l_y}{2}}\int_{-\frac{l_x}{2}}^{\frac{l_x}{2}}|V|dxdy \end{aligned} \tag{7}$$

The loss of power on the left sole is the same as that on the right since the left-foot motion is symmetrical to the right-foot motion about the origin of the base frame of the robot. Substituting (5) into (7), we obtain the total loss of power on the both soles $\mathcal{P}$:

$$\begin{aligned} \mathcal{P} &= 2\mathcal{P}_{right} \\ &= \mu Mg\int_{-\frac{l_y}{2}}^{\frac{l_y}{2}}\int_{-\frac{l_x}{2}}^{\frac{l_x}{2}}|V| \; dxdy \\ &= \mu Mg\int_{-\frac{l_y}{2}}^{\frac{l_y}{2}}\int_{-\frac{l_x}{2}}^{\frac{l_x}{2}}\sqrt{V^2} \; dxdy \end{aligned} \tag{8}$$

In order to calculate ω that would minimize $\mathcal{P}$, we proceed as follows. Differentiating (8) with respect to ω yields:

$$\frac{\partial\mathcal{P}}{\partial\omega} = \mu Mg\frac{\partial}{\partial\omega}\int_{-\frac{l_y}{2}}^{\frac{l_y}{2}}\int_{-\frac{l_x}{2}}^{\frac{l_x}{2}}\sqrt{V^2}dxdy \tag{9}$$

Since ω that would minimize $\mathcal{P}$ requires (9) to be zero, we obtain:

$$\frac{\partial}{\partial\omega}\int_{-\frac{l_y}{2}}^{\frac{l_y}{2}}\int_{-\frac{l_x}{2}}^{\frac{l_x}{2}}\sqrt{V^2}dxdy = 0 \tag{10}$$

Because this equation contains neither the friction coefficient nor the total mass of the robot nor the gravity acceleration, the shape of the sole and a given motion pattern alone decide the rotation of the robot. This also implies that the friction coefficient does not affect the rotation.

Equation 10 can also be described by the square of V as follows:

$$\begin{aligned} &\mathcal{P}^* \\ &= \int_{-\frac{l_y}{2}}^{\frac{l_y}{2}}\int_{-\frac{l_x}{2}}^{\frac{l_x}{2}} V^2 dxdy \\ &= \int_{-\frac{l_y}{2}}^{\frac{l_y}{2}}\int_{-\frac{l_x}{2}}^{\frac{l_x}{2}} \{v_x + \omega|Y_B + y|\}^2 \\ &\qquad + \{v_y + \omega|X_B + x|\}^2 \; dxdy \\ &= \{v_x^2 + v_y^2 + 2v_x Y_B\omega + 2v_y X_B\omega \\ &\quad + \omega^2(X^2 + Y^2) + \frac{\omega^2}{12}(l_x^2 + l_y^2)\}l_x l_y \end{aligned} \tag{11}$$

$$\begin{aligned} &\frac{\partial\mathcal{P}^*}{\partial\omega} \\ &= \{2\omega(X^2 + Y^2) + \frac{\omega}{6}(l_x^2 + l_y^2) + 2v_x Y_B + 2v_y X_B\}l_x l_y \\ &= 0 \end{aligned} \tag{12}$$

Finally we obtain:

$$\omega = -\frac{12(Y_B v_x + X_B v_y)}{12(X_B^2 + Y_B^2) + l_x^2 + l_y^2} \tag{13}$$

Equation 13 relates the given velocity $\boldsymbol{v}(v_x, v_y)$ to the angular velocity ω due to the friction torque. Note that the rotation has no relation to the friction coefficient. It is also important that the surface of the soles affects the rotational angle: The smaller the foot, the larger the rotational angle. It may give the reason why humans often stand on their toes when they twirl in place, as already shown in Fig. 1.

B. Asymmetric load on the feet

The hypothesis that we proposed above is also used in the case where the robot's load is asymmetrically distributed between the right and left feet. In Fig. 5, the motion of the both feet is shown for explaining the hypothesis. In the generated motion patterns, the positions of the right and left feet are always homothetic with respect to the COP, and the ratio between the distances of the right and left feet from the COP is expressed as $\alpha : 1-\alpha$ $(0 \leq \alpha \leq 1)$. The distance between the feet is $2X_B$ along the x-axis and $2Y_B$ along the y-axis of the base frame.

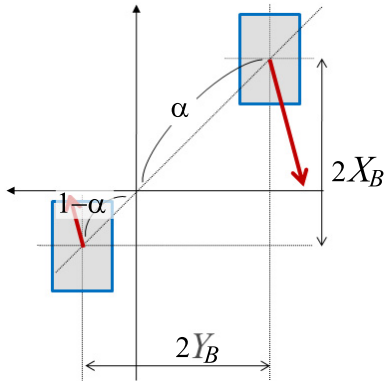

Fig. 5. Asymmetric load's model. COP is assumed to be at the origin of the projection of the robot's base frame on the floor.

The total loss of power at the both soles is expressed as follows:

$$\mathcal{P} = \int_{-\frac{l_y}{2}}^{\frac{l_y}{2}} \int_{-\frac{l_x}{2}}^{\frac{l_x}{2}} f_{right} V_{right} + f_{left} V_{left} \; dxdy \quad (14)$$

where V_{right} and V_{left} represent the velocities of the right and left feet, and f_{right} and f_{left} denote the applied load to the right and left feet, respectively. The velocities of the feet are defined as follows:

$$\begin{aligned} V_{right} &= \sqrt{V^*_{right}} \\ V^*_{right} &= \{2\alpha v_x + \omega|2\alpha Y_B + y|\}^2 \\ &\quad +\{2\alpha v_y + \omega|2\alpha X_B + x|\}^2 \\ V_{left} &= \sqrt{V^*_{left}} \\ V^*_{left} &= \{2(1-\alpha) v_x + \omega|2(1-\alpha) Y_B + y|\}^2 \\ &\quad +\{2(1-\alpha) v_y + \omega|2(1-\alpha) X_B + x|\}^2 \end{aligned} \quad (15)$$

If the load can be assumed to be also proportional to α, f_{right} and f_{left} can be expressed as follows:

$$\begin{aligned} f_{right} &= \mu M g(1-\alpha) \\ f_{left} &= \mu M g \alpha \end{aligned} \quad (16)$$

Substituting (15) and (16) into (14), ω can also be obtained that would minimize $\mathcal{P}$ in (14). However, the expression obtained by differentiating and solving (14) with respect to ω is complicated. Therefore, we calculate ω numerically in the next section of this paper.

III. EXPERIMENTS WITH HUMANOID HRP-2

In this section, we execute three experiments.

1) Turn with a different friction coefficient μ.
2) Symmetric turn with a different initial stance X_B.
3) Asymmetric turn with a different COP position (different α).

Figure 6 shows the given motion of the feet. On the left-hand side in the figure, the dotted boxes represent the positions of the feet at the beginning of the motion. The robot stands with its feet $2X_B$ apart along the x-axis, and $2Y_B$ apart along the y-axis of the base frame. It moves them

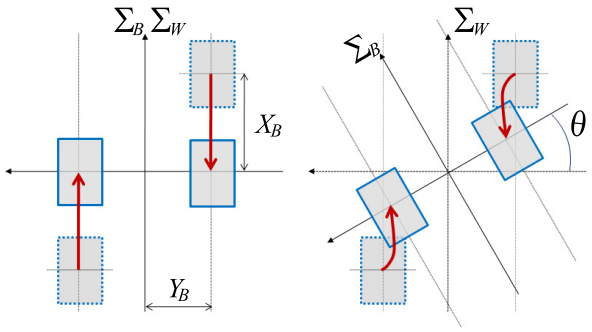

Fig. 6. Motion of both feet. Left: given pattern. Right: expected motion. The rotational torque may be produced by friction force.

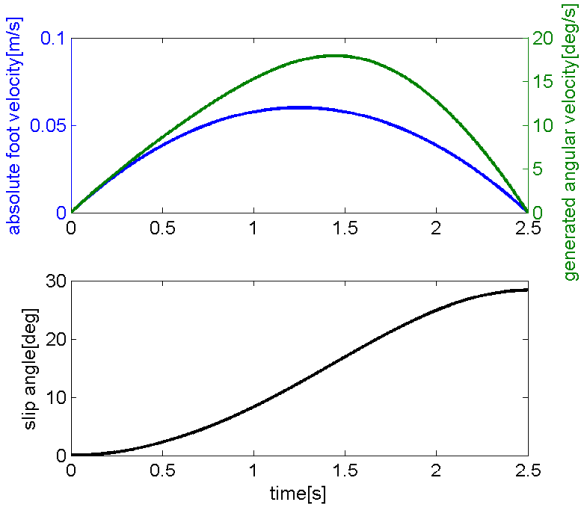

Fig. 7. Planned foot velocity, expected angular velocity (ω), and rotational angle (θ) resulting from slip

according to the arrows and reaches the positions represented with solid boxes. The given trajectories of the feet are both parallel to the x-axis with a distance of $Y_B = Y_{init}$. The applied force may rotate the robot body in the opposite direction due to the reaction force. The expected final positions of the feet are shown on the right-hand side in Fig. 6. To generate the motion patterns of HRP-2, we used OpenHRP developed in the Humanoid Robotics Project(HRP) [20]. The generated trajectory is shown in Fig. 7. In experiments on asymmetric turn also, the same trajectory of the feet was adopted, but the position of the COP is not in the middle of both feet.

In order to obtain low friction, small plastic plates were set on two sides of the soles of HRP-2, where contact with a floor, as shown in Fig. 8, and a large sheet was set on the floor. The friction coefficient between the plastic sheets set on the sole and floor was 0.1. These sheets were used because the soles of HRP-2 were covered with a rubber-like material. The friction coefficient of the rubber soles were $\mu > 1.0$ on the lab floor, which might have caused an excessive load on the motor of the robot when the feet rub against the floor.

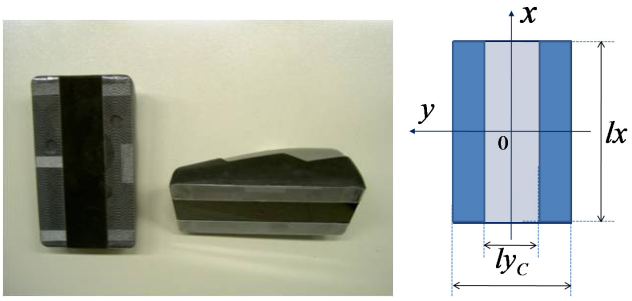

Fig. 8. Left: feet of HRP-2, fitted with plastic plates. Right: foot of HRP-2. The values l_x, l_y, and l_{y_c} are the same as those of real HRP-2's foot.

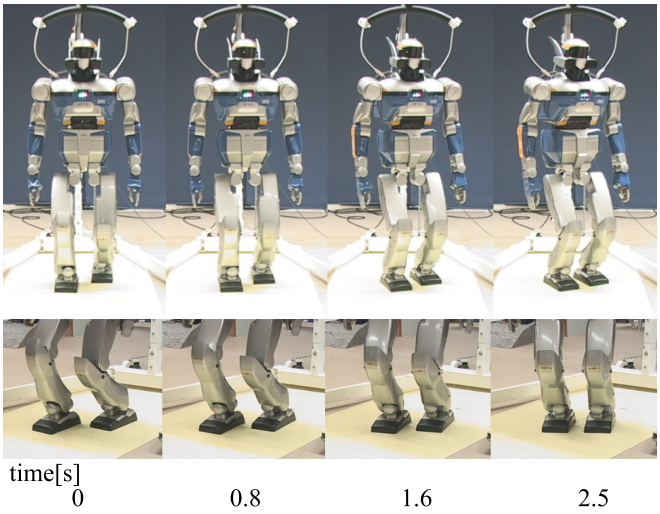

Fig. 9. Experiment: time-line of foot motion of HRP-2 slipping and turning on the low friction floor.

A. Comparison between different friction coefficients

In order to confirm the prediction that the friction coefficient does not affect the rotational angle when a robot turns by slipping the feet, an experiment was performed with the humanoid HRP-2. The motion of the robot was symmetric, as shown in Fig. 6, and the robot stood with its feet $2X_B$ apart along the x-axis, and $2Y_B$ apart along the y-axis of the base frame in the initial posture, where $X_B = \{0.10, 0.08, 0.06, 0.04, 0.02\}[m]$, and $Y_B = 0.095[m]$. Further, in order to obtain a different friction coefficient, the plastic placed on the two sides of the soles were removed. The friction coefficient between the plastic sheet on the floor and the rubber sole of HRP-2 was 0.3, as against 0.1 between two plastic sheets.

The test has been conducted five times for each condition of the initial stance and friction coefficient. Figure 9 shows a sequence of photographs of the feet of HRP-2. Figure 10 illustrates the results of the experiment. Straight-line approximations are also plotted on the figure. The slopes of these fitted lines agree well with each other, and their approximations are: $\theta = 315.2X_B$ for $\mu = 0.3$, and $\theta = 320.3X_B$ for $\mu = 0.1$. It turns out that friction coefficient makes no difference to rotational angle in this case.

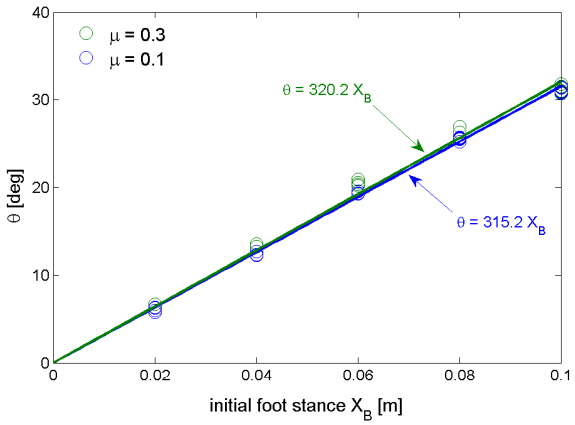

Fig. 10. Experimental results: rotational angle produced by slip turn with different friction coefficients. The blue circles and the line indicate the results for slip angle and fitted line with $\mu = 0.1$, and the green circles and the line are for $\mu = 0.3$.

B. Comparison between different stances

In the experiment, the robot was made to move the feet back and forth through various distances. Since the motion of the robot was also symmetric, as shown in Fig. 6, and the feet trajectory had a constant stance in the y-axis direction, our hypothesis in (13) can be simplified:

$$\omega = -\frac{12Y_{init}v_x}{12(X_B^2 + Y_{init}^2) + l_x^2 + l_x l_{yc} + l_{yc}^2 + l_y^2} \quad (17)$$

where l_{yc} is the distance between small plastic plates placed on the soles, as shown in Fig. 8

The initial position of the right foot varies over $X_B = \{-0.10, -0.08, -0.06, -0.04, -0.02, 0.02, 0.04, 0.06, 0.08,$

$0.10\}[m]$. The sideway distance between the feet was maintained to be $Y_{init} = 0.095[m]$. The rotational angle of the body about the vertical axis is measured at the final position. The test has been conducted five times for each condition of initial stance. Figure 11 illustrates the results; the comparison between the results obtained through the hypothesis and the experiment. The results shown in the figure indicate that the proposed hypothesis can be used for predicting the amount of the rotational angle from a generated motion pattern. However, the larger the initial foot positions, the larger the error between them. Because all motions are performed in $2.5[s]$, a wide initial foot stance induces a large velocity of motion and a large inertial force. This is thought to be the cause of the error from the hypothesis.

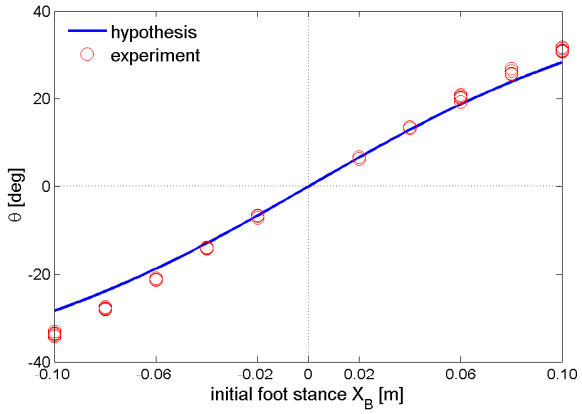

Fig. 11. Experimental results: rotation angle by slip turn.

C. Comparison between different positions of COP

In the experiment, the robot's COP took different positions. The position expressed by α in (14) varies over $\alpha = \{0.00, 0.125, 0.250, 0.500, 0.625, 0.750, 0.825, 1.00\}$. The start position of the right foot was $X_B = 0.1[m]$ throughout the experiment. The sideway distance between the feet was also maintained to be $Y_{init} = 0.095[m]$. The experiment was conducted five times for each value of α.

The expectancy by the hypothesis has been calculated numerically because the solution ω that minimize (14) is very complicated. Figure 12 shows the results of the calculated expectancy according to (14) that obtained on the basis of the hypothesis, and the experimental result with a humanoid robot HRP-2.

There is a large difference between the calculated expectancy and the experimental results. It is attributed to the difference of the mass distribution between the model and the real robot. Although we first assumed that the COP and the origin of the base frame of the robot model coincide each other, HRP-2 has asymmetric mass distribution. Moreover the real-time stabilizing system of HRP-2 affects the position of its COP. Since α expresses the ratio between the distances of the right and left feet from the COP, the incorrect position of COP leads the error of (14).

In order to obtain the correct value of the rotational angle θ, it is necessary to use the real value of α. The ratio of the floor reaction force acting on the right foot of HRP-2 to the total floor reaction force is illustrated in Fig. 13. It is

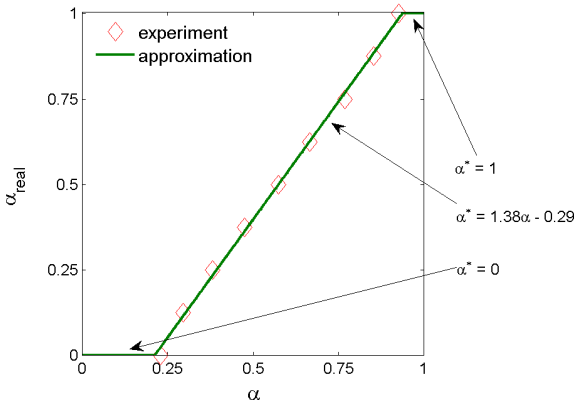

Fig. 13. Real ratio between the distances of the right and left feet from the COP (α_{real}). The green line signifies the straight-line approximation of α_{real}.

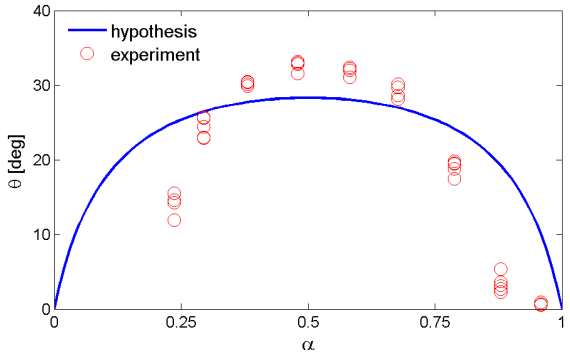

Fig. 12. Rotational angle θ calculated numerically according to the hypothesis, and the experimental results with HRP-2.

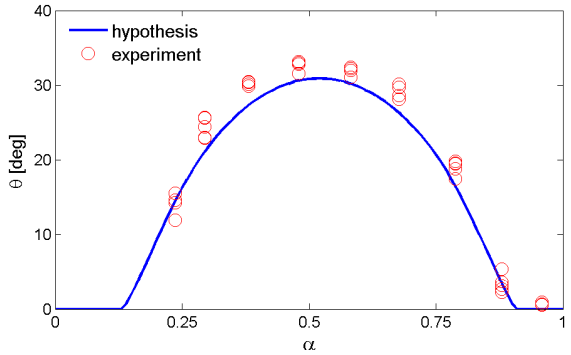

Fig. 14. Rotational angle θ calculated numerically according to the hypothesis with α^*, and the experimental results for comparison.

in direct proportion to the position of the COP and is hence equivalent to real α.

$$\alpha_{real} = \frac{Fz_{left}}{Fz_{right} + Fz_{left}} \quad (18)$$

where, Fz_{right} and Fz_{left} signify the floor reaction force detected by the force sensors on the right and left foot of HRP-2, respectively. The real ratio between the distances of the right and left feet from the COP is approximated as follows:

$$\alpha^* = \begin{cases} 0 & \text{if } 0 \leq \alpha < a_{lower} \\ \frac{\alpha - a_{lower}}{a_{upper} - a_{lower}} & \text{if } a_{lower} \leq \alpha < a_{upper} \\ 1 & \text{if } a_{upper} \leq \alpha \end{cases} \quad (19)$$

The thresholds in the case of Fig. 13 are determined to be $a_{lower} = 0.21$ and $a_{upper} = 0.94$.

By substituting α^* in (19) into α in (14), (15), and (16), we find that our hypothesis agrees well with the experiment with HRP-2, as shown in Fig. 14.

IV. CONCLUSIONS AND FUTURE WORKS

A discussion on twirling a humanoid robot by utilizing the slip between the feet and the ground was presented. To generate the slip motion, we predict the amount of slip under the hypothesis that turning motion is caused by the effect of minimizing the power generated by floor friction. We also conducted experiments with a humanoid robot HRP-2 in order to verify the proposed hypothesis.

The results for the different values of the friction coefficient indicated that the friction coefficient does not affect the rotational angle of the robot. In addition, from the results obtained under the symmetric load distribution between the feet and for different feet positions, it can be said that the proposed hypothesis agrees with the experiment, and is hence adequate to predict the amount of a slip turn of a robot. However, an error between the hypothesis and the experimental results occurred when the sideway distance between the feet in the initial stance was widened. This may due to a large velocity of motion that induces non-negligible inertial force. The results for an asymmetric load did not agree well with the hypothesis under the assumption that the COP and the origin of the base frame coincide with each other. On the other hand, once correct floor reaction force was incorporated in our hypothesis, the hypothesis is quite adequate to predict the amount of slip even in the case of an asymmetric load.

Because of the few DOFs and the limited joint range of HRP-2, it is impossible to stand HRP-2 on the toes so as to reduce the ground contact area or to twist its leg as much as a human. Furthermore, humans utilize inertial force by twisting the upper body and swinging the arms. Future study will also address this effect in order to achieve highly sophisticated human-like motion.

REFERENCES

[1] L. Strandberg, "On accident analysis and slip-resistance measurement," *Ergonomics*, vol. 26, no. 1, pp. 11–32, 1983.

[2] M. Redfern and B. Bidanda, "Slip resistance of the shoe-floor interface under biomechanically-relevant conditions," *Ergonomics*, vol. 37, no. 3, pp. 511–524, 1994.

[3] J. Hanson, M. Redfern, and M. Mazumdar, "Predicting slips and falls considering required and available friction," *Ergonomics*, vol. 42, no. 12, pp. 1619–1633, 1999.

[4] R. Brady, M. Pavol, T. Owings, and M. Grabiner, "Foot displacement but not velocity predicts the outcome of a slip induced in young subjects while walking," *Journal of Biomechanics*, vol. 33, pp. 803–808, 2000.

[5] G. Boone and J. Hodgins, "Reflexive responses to slipping in bipedal running robots," in *Proc. IEEE International Conference on Intelligent Robots and Systems*, 1995, pp. 158–164.

[6] ——, "Slipping and tripping reflexed for biped robots," *Autonomous robots*, vol. 4, pp. 259–271, 1997.

[7] J. Park and O. Kwon, "Reflex control of biped robot locomotion on a slippery surface," in *Proc. IEEE International Conference on Robotics and Automation*, 2001, pp. 4134–4139.

[8] S. Kajita, K. Kaneko, K. Harada, F. Kanehiro, K. Fujiwara, and H. Hirukawa, "Biped walking on a low friction floor," in *Proc. IEEE International Conference on Intelligent Robots and Systems*, 2004, pp. 3546–3552.

[9] M.Vukobratović and J.Stepanenko, "On the stability of anthropomorphic systems," *Mathematical Biosciences*, vol. 15, pp. 1–37, 1972.

[10] K. Kaneko, F. Kanehiro, S. Kajita, H. Hirukawa, T. Kawasaki, M. Hirada, K. Akachi, and T. Isozumi, "Humanoid robot hrp-2," in *Proc. IEEE International Conference on Robotics and Automation*, 2004, pp. 1083–1090.

[11] K. Kaneko, F. Kanehiro, S. Kajita, M. Morisawa, K. H. Kiyoshi Fujiwara, and H. Hirukawa, "Slip observer for walking on a low friction floor," in *Proc. IEEE International Conference on Intelligent Robots and Systems*, 2005, pp. 1457–1163.

[12] C. Zhu and A. Kawamura, "What is the real frictional constraint in biped walking? - discussion on frictional slip with rotation -," in *Proc. IEEE International Conference on Intelligent Robots and Systems*, 2006, pp. 5762–5767.

[13] M. Nishikawa, Japanese Patent P2005-238 407A, Sept. 8, 2005.

[14] ——, Japanese Patent P2007-326 169A, Dec. 20, 2007.

[15] M. Koeda, T. Yoshikawa, and T. Ito, "Stability improvement by slip-based turning motion of humanoid robot," in *Proc. 25th Annual Conference of the RSJ*, no. 3H15, 2007, (in Japaqnese).

[16] M. Koeda, T. Ito, and T. Yoshikawa, "Shuffle turn with both feet of humanoid robot by controlling load distribution of soles," in *Proc. 12th International Conference on Climbing and Walking Robots and the Support Technologies for Mobile Machines (CLAWAR2009)*, 2007, pp. 1007–1014.

[17] K. Miura, M. Morisawa, S. Nakaoka, K. Harada, and S. Kajita, "A friction based "twirl" for biped robots," in *Proc. 8th IEEE-RAS International Conference on Humanoid Robots*, 2008, pp. 279–284.

[18] K. Harada, "Pushing manipulation for multiple objects," *Trans. of the ASME*, vol. 128, pp. 422–427, 2006.

[19] K. Lynch, "Estimating the friction parameters of pushed objects," in *Proc. IEEE International Conference on Intelligent Robots and Systems*, 1993, pp. 186–193.

[20] H. Hirukawa, F. Kanehiro, and K. Yokoi, "Hrp develops openhrp," in *IEEE/RSJ IROS Workshop on exploration towards Humanoid Robot Applications*, 2001.